Reprinted from the *Soil Science Society of America Journal*
Volume 54, no. 3, May–June 1990
677 South Segoe Rd., Madison, WI 53711 USA

In Situ Measurements of Soil Physical Properties by Acoustical Techniques

J. M. Sabatier, H. Hess, W. P. Arnott, K. Attenborough, M. J. M. Römkens, and E. H. Grissinger

In Situ Measurements of Soil Physical Properties by Acoustical Techniques

J. M. Sabatier,* H. Hess, W. P. Arnott, K. Attenborough, M. J. M. Römkens, and E. H. Grissinger

ABSTRACT

Knowledge of porosity, air permeability, pore structure, and surface layering of soils is desirable in agricultural research. The conventional techniques are invasive, typically requiring sample extraction. When monitoring seasonal changes, the conventional methods disrupt considerable proportions of the test plot surface. The sample area used in conventional measurements may be too small to represent the variations in the test plot. Here, the feasibility of acoustical techniques for monitoring surface air porosity (total porosity minus volumetric water content), air permeability, and pore structure and the variation of these properties to depths of several centimeters below the surface is demonstrated. Test soil plots prepared using three soil materials, masonry sand, a Grenada silt loam (fine-silty, mixed, thermic Glossic Fragiudalf) and a Catalpa silty clay (fine, montmorillonitic, thermic Fluvaquentic Hapludoll), were considered. Variation in water content and compaction of each soil material were considered. Both acoustic reflection and transmission measurements were made in the audio-frequency range. The soils are modeled as air-filled, rigid-framed porous media. The acoustic-reflection measurements involve analysis of propagation data from a small loudspeaker and two vertically separated microphones. The acoustic-transmission measurement requires a specially designed probe microphone. Analysis of the acoustic-reflection data yields qualitative indications of the relative air permeability of the soils. The transmission measurement yields information about the changes in air permeability with depth. Quantitative information on surface porosity, air permeability, tortuosity, and layering is presented by fitting theoretical predictions based on the soil model to the measured sound reflection and transmission data. The acoustically determined air porosity for the soils considered is within 10% of the values determined by gravimetric techniques.

IN AGRICULTURAL RESEARCH, a knowledge of air-filled and air-connected pores, porosity and pore-size distribution, air permeability, soil water content, and near-surface layering is desirable to indicate the soil structure, compaction, and aeration. The precise relationship between these indicators and crop yields is not fully understood. Nevertheless, it is clear that pore structure, low air content, and low air and water permeability often associated with heavily wheeled sites will inhibit seed germination and affect root development, water intake, and, ultimately, crop yields as well as erosion and run-off processes.

The gravimetric technique of measuring percentage volumes of water and air in the pores is destructive, labor intensive, and slow, and is particularly difficult on clay soils due to swelling and shrinking effects (Hillel, 1982). Porous plate, sand table (Van der Haarst and Stakman, 1965), and pressure membrane cell (Avery and Bascombe, 1982) techniques may take several days and, consequently, include the risk of air entrapment. Air entrapment may render the assumption of complete water saturation invalid (Vomocil, 1965). These techniques are also unsuitable for soil samples that swell and shrink on wetting and drying (Page, 1948). The air pycnometer (Kummer and Cooper, 1945; Russell, 1950; Pidgeon, 1974) and porosimeter (Janse, 1969, p. 89–123) are relatively fast techniques, after lengthy calibrations for particular sample holders, but require recalibration daily because of atmospheric pressure and temperature changes. In situ, the pressure pycnometer acts like a gas-filled thermometer and necessitates rapid reading and shading (Vomocil, 1965).

If any of these techniques are used to monitor changes in porosity throughout the season, then it is necessary to extract core samples repeatedly from the trial plot of interest. This will disrupt a considerable proportion of the plot surface and reduce the area available for subsequent monitoring. Moreover, core samples are difficult to extract where the soil is loose or stony.

Laboratory-based measurements of air permeability (Leonard, 1946) also require extraction of core samples. In addition to disturbance during extraction, samples may be further disturbed during subsequent transport. In situ permeameters (Kirkham, 1947; Grover, 1955) involve insertion of a sampling container and may involve surface sealing with paraffin wax or wallpaper paste. These systems involve problems of unknown sample length, disturbance of natural soil condition, and repeatability, particularly

J.M. Sabatier, H. Hess, and W.P. Arnott, Natl. Center for Physical Acoustics, P.O. Box 847, Univ. of Mississippi, University, MS 38677; K. Attenborough, Dep. of Physics and Astronomy, Univ. of Mississippi, University, MS 38677; and M.J.M. Römkens and E.H. Grissinger, USDA Sedimentation Lab., P.O. Box 1157, Airport Rd., Oxford, MS 38677 (H. Hess and K. Attenborough on leave from the Dep. of Engineering Mechanics, The Open Univ., Walton Hall, Milton Keynes MK7 6AA, England.) Received 15 June 1989. *Corresponding author.

Published in Soil Sci. Soc. Am. J. 54:658–672 (1990).

where permeability changes are being monitored over a growing season. Permeability measurements that force air through a sample must take account both of drying effects and the onset of turbulence. The former consideration suggests rapid reading and rapid air flow, whereas the latter consideration makes low air speeds preferable. The relatively small sample size used in conventional permeability measurements may be too small to represent the contribution of macropores or surface cracks to permeability.

These conventional techniques are frequently inadequate to measure the structure, depth, and air permeability of surface seals and crusts associated with rain. Penetrometers may be used to study compaction with depth, as they indicate more resistant layers. However, the fragility and finite thickness of surface crusts limit the success of penetrometer measurements. Moreover, there is no standard design or procedure for penetrometer measurements and they yield only qualitative indications of density, shear strength, and load bearing (mechanical impedance) rather than air flow or porosity (hydraulic impedance).

Acoustical techniques are feasible for monitoring surface air porosity, air permeability, and tortuosity and the variation of these properties down to depths of several centimeters below the surface. These techniques involve measurements of both the reflection and transmission of audio-frequency broadband sound by the soil. Sound-reflection measurements are relatively noninvasive, may be made in situ and may be used alone to give qualitative indications of relative air permeability of different homogeneous soils and to monitor effects of changes in soil water content and weathering on a particular soil. The reflection measurements involve analysis of short-range propagation from a loudspeaker source to a pair of vertically separated microphones (Fig. 1a). Sound-transmission measurements are made with a buried (probe) microphone (Fig. 1b). The probe-microphone measurements give direct indications of qualitative changes in air permeability with depth. Hence, these measurements may be used to indicate either the thickness of surface crusts or the presence of plow or compaction pans within a few centimeters of the soil surface.

Quantitative information on surface porosity and air permeability is given by fitting theoretical predictions based on a homogeneous-soil model to the measured sound-reflection data on soils. A similar approach can be used, along with the probe-microphone data, to give quantitative information about nonuniformity or heterogeneity of soils. These acoustical techniques have been validated by preparation of and measurements on a series of carefully prepared trial plots containing sand, clay, and loess soils (Fig. 1c,d).

MATERIALS AND METHODS

Physics of Sound Reflection and Transmission

When airborne sound is incident on the surface of a soil, air contained by connected pores in the soil oscillates in and out of the pores. The resulting area-average volume flow is governed both by the frequency and amplitude of the sound waves and by the properties of the soil. The coupling of energy of the vibrating air above the soil surface with the

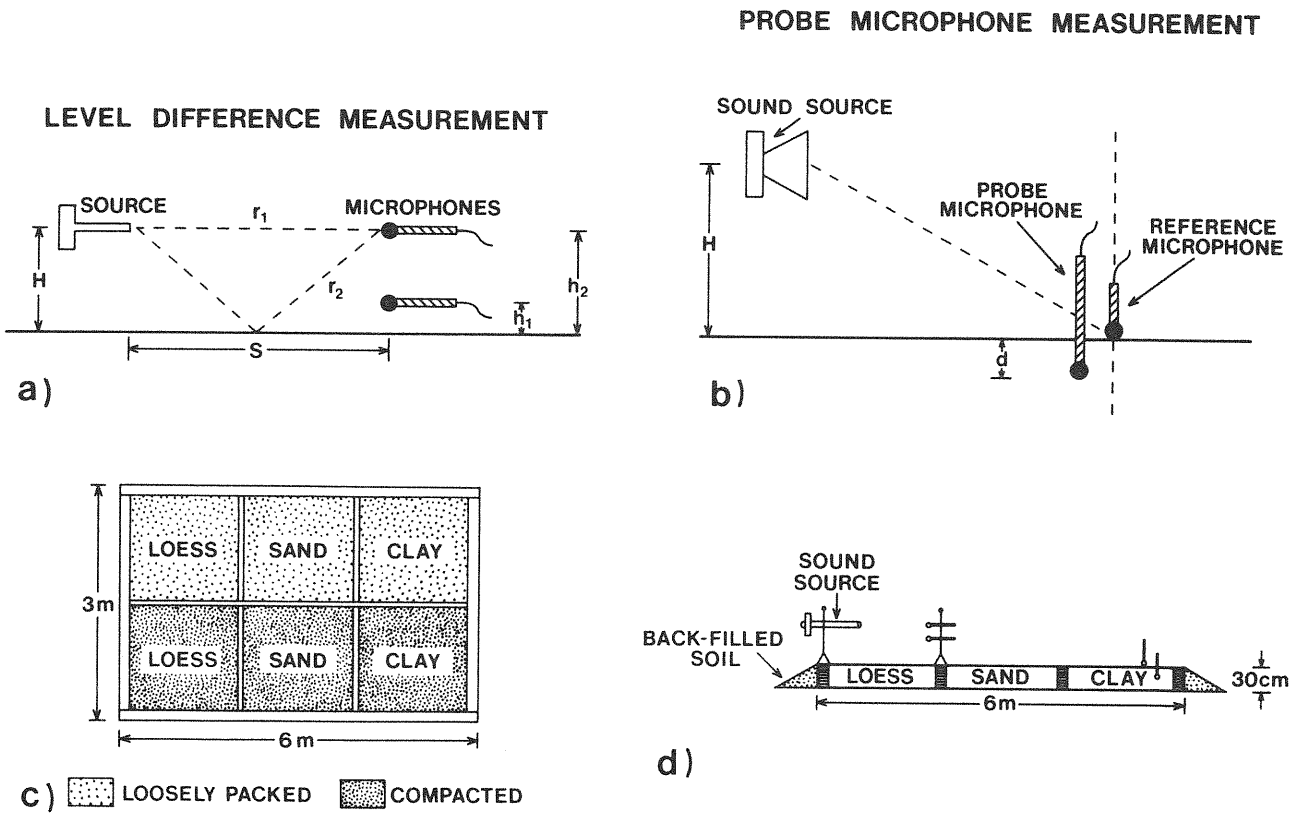

Fig. 1. a. Schematic diagram of acoustic level difference measurement. b. Schematic diagram of probe measurement. c. Top view of soil plots. d. Cross section of test plots.

air in the soil pores and, hence, the penetration of the sound waves is strong if the air permeability is high. Conversely, low air permeability means weak coupling and little sound penetration. The transmitted sound is attenuated by viscous friction at the walls of the pores. In addition to macroscopic parameters such as air porosity and air permeability, the microstructure of the pores has an important influence on both the speed and attenuation of the penetrating sound waves. These microstructural parameters include characteristic pore shape, pore-size distribution, tortuosity, changes in cross-sectional area of the pores, and intersections of pores along their length. A pore structure with increased effective surface area (pore shape and size) or effective length of the pore per unit depth (tortuosity) will decrease the sound speed and increase the attenuation, or absorption, of sound.

Discrete changes in porosity and permeability as a function of depth within the soil will result in reflections of the penetrating sound, which will influence the amplitude and phase of both the sound waves travelling upwards from the soil surface and those penetrating through the soil layers.

Previous theoretical work has shown that the acoustical behavior of a porous granular medium may be described in terms of its porosity, air-flow resistivity, pore shape, and tortuosity (Attenborough, 1983, 1985). Air-flow resistivity is defined by the ratio of the kinematic viscosity of air and the air permeability. Strictly, sound incident on the surface of a soil will excite motion in the solid soil particles as well as in the air in the pores. In other words, there are poroelastic effects. Theoretical and experimental work has shown that, for the range of sound frequencies of 10^2 Hz to 10^4 Hz and during analysis of the specific measurements of interest, these poroelastic effects may be ignored (Sabatier et al., 1986; Attenborough et al., 1986). Furthermore, for this frequency range, acceptable approximations for the acoustical parameters involve only three parameters: the porosity of air-filled connected pores, Ω; the tortuosity, T; and an effective flow resistivity, σ_{eff} (Hess, 1988). The latter parameter is related to the actual flow resistivity (σ) according to $\sigma_{eff} = \Omega S_p^2 \sigma$ where S_p is a pore-shape factor.

Acoustical properties of porous media that are sufficient to describe both sound reflection and sound transmission are the relative characteristic impedance, Z, and the propagation constant, k (Kinsler et al., 1980; Morse and Ingard, 1986). The quantity Z is the product of complex density and complex sound speed in the porous media divided by the same product for sound in air. The k is the quantity $2\pi f$ divided by the complex sound speed in the porous media where f is the sound-wave frequency. The real part of k is $2\pi f$ divided by the phase speed and the imaginary part is the attenuation constant. The use of complex quantities is a convenient way of including attenuation. The approximate relationship (Attenborough, 1985) for k derived from a capillary model of the soil microstructure with adjustments for arbitrary pore shape (pore-size distribution) and tortuosity is

$$k \simeq 0.0079 \sqrt{f}\,[8.14Tf + i4\sigma_{eff}]^{0.5} \qquad [1]$$

where i is the square root of -1. The real part of this has units m^{-1} and the imaginary part has units of nepers m^{-1} (Kinsler, et al., 1980). (Attenuation coefficients for waves decaying with distance are frequently expressed in nepers m^{-1}. Note that the neper is a dimensionless unit.) Also, Z (Attenborough, 1985) is given by

$$Z \simeq 0.0029[1.33T + i0.531\sigma_{eff}/(\Omega^2 f)]/(\Omega k). \qquad [2]$$

The speed of sound in air and the density of air have been assumed to be 343 m s^{-1} and 1.2 kg m^{-3}, respectively, in obtaining the numerical constants in Eq. [1] and [2]. These values of air sound speed and density are appropriate for an atmospheric temperature of 20 °C and atmospheric pressure of 10^5 Pa.

Equation [2] may be used to obtain the plane-wave reflection coefficient, R (Kinsler et al., 1980; Officer, 1958) for sound incident at an angle ψ to the vertical on a homogeneous soil:

$$R = \frac{Z\cos\psi - 1}{Z\cos\psi + 1}. \qquad [3]$$

Plane waves are difficult to obtain experimentally for in situ measurements; consequently, a more useful quantity is the spherical-wave reflection coefficient:

$$Q \simeq R + (1 - R)F(f,\psi,Z). \qquad [4]$$

Useful expressions and approximations for $F(f,\psi,Z)$, which acts as a correction for wave-front sphericity, are well known and may be found in detail elsewhere (Chien and Soroka, 1980). Appendix A contains a further discussion of $F(f,\psi,Z)$.

The complex form of both the plane-wave and spherical-wave reflection coefficients is the result of phase and amplitude changes of incident sound waves following reflection at a soil surface. Consider a broadband omnidirectional sound source placed near a soil surface. The amplitude spectrum measured with a microphone at a similar height and some distance from the source exhibits several minima resulting from interference between the direct and reflected wave components (Pierce, 1981; Officer, 1958). The first minimum is associated mainly with the wave's phase change on reflection and, consequently, is sensitive to ground impedance (Attenborough, 1985; Hess, 1988; Attenborough and Hess, 1985). Hence, the frequency location and form of this first minimum in the measured amplitude spectrum are sensitive indicators of the soil physical properties. Equations [2] through [4] suggest that acoustical measurements may be used to deduce Ω, σ_{eff}, and T.

Rather than working with the measured amplitude spectrum, it is usual to remove the effect of wave-front spreading by dividing the measured amplitude spectrum by that measured in the absence of the reflecting ground, which is known as the free-field amplitude spectrum. The free-field spectrum requires an anechoic environment for its measurement. It is more convenient to partially remove the effect of wave-front spreading by dividing the measured amplitude spectrum at an elevated microphone by that obtained at another microphone placed on or near the ground surface (Fig. 1a).

Again, the frequency location and form of the first minimum in this acoustic-level (or amplitude) difference spectrum are indicators of the soil physical properties. Figure 2a illustrates the theoretical variation in the level difference spectrum with σ_{eff} for a typical measurement geometry. As the σ_{eff} is increased, the first minimum in the level difference spectrum is shifted to higher frequencies and deepened. Variation in the porosity and tortuosity has a less major effect on the first dip but a more significant effect at higher f. Appendix A discusses the calculation of the acoustic-level difference spectrum.

Equation [1] indicates that the phase speed and attenuation of sound penetrating through a soil surface are dependent on the σ_{eff} and on f. Indeed, as either quantity increases, so does the attenuation and the phase change with depth (d). At $f < 500$ Hz, typical speeds of sound penetrating the pores of a soil are so much smaller than the speed of sound in air that whatever angle sound is incident it is strongly refracted towards the normal at the air-soil boundary. For this case of strong refraction, a useful approximation for the sound fields below and at the surface (Richards et al., 1985) is

$$\frac{\text{complex pressure at surface}}{\text{complex pressure at depth } d} \simeq \exp(ikd), \qquad [5]$$

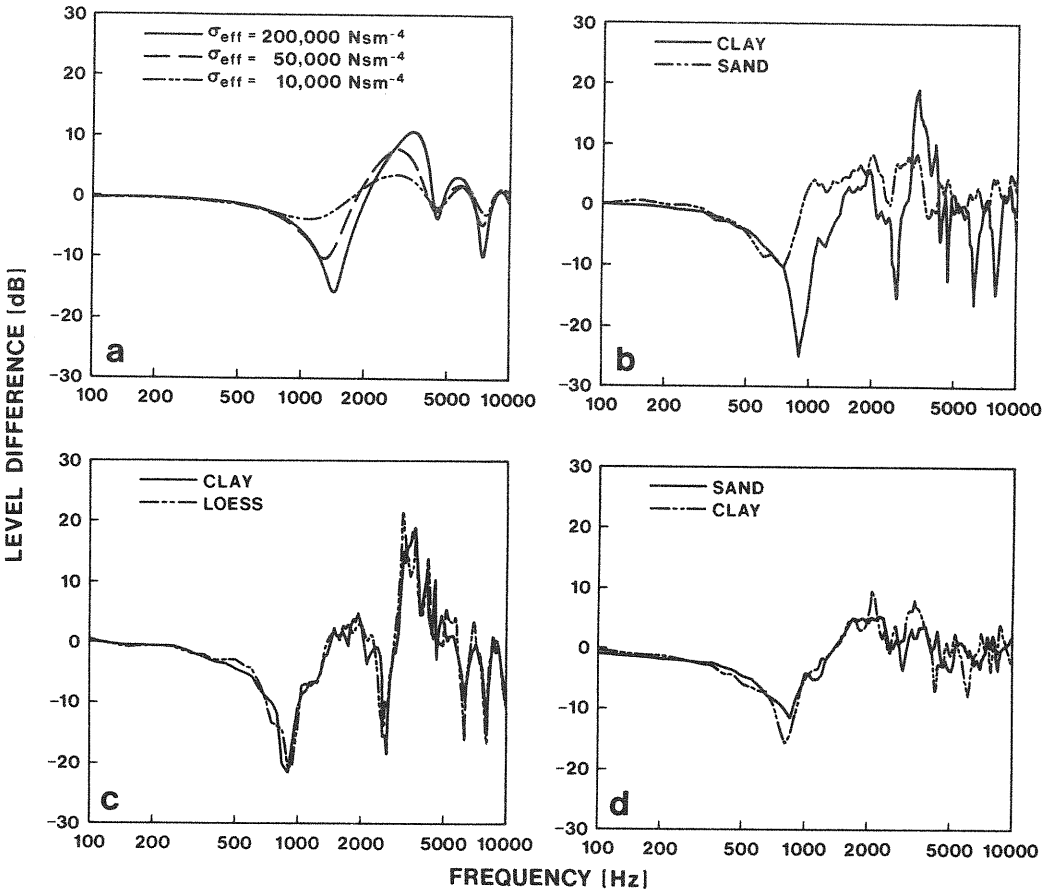

Fig. 2. a. Theoretical effect of variation in flow resistivity on the level difference spectrum. Geometrical parameters (see Fig. 1a) are $H = 0.3$ m, $S = 1.6$ m, $h_1 = 0.1$ m, and $h_2 = 0.3$ m. Acoustical parameters are tortuosity = 3.0, porosity = 0.4, and the values of effective flow resistivity (σ_{eff}) given on the figure. b. Measured level difference spectra over intermediate, loosely packed sand and wet, compacted clay. c. Measured level difference spectra over wet, loosely packed loess and clay. d. Measured level difference spectra over dry, loosely packed clay and sand.

where complex pressure includes both phase and magnitude. Approximation [5] is used to compute the attenuation and phase of the acoustic wave at the probe microphone relative to that of the reference microphone (Fig. 1b). Hence, if, at a given frequency,

$$k = a + ib \qquad [6]$$

where a is known as the phase constant and b as the attenuation constant, given by the real and imaginary parts of Eq. [1], then the attenuation (in dB) with depth may be calculated from

$$\text{attentuation} = \frac{20\,bd}{\log_e 10} \qquad [7]$$

and the phase change ($\Delta\phi$ in degrees) with depth is given by

$$\Delta\phi = \frac{180}{\pi} ad. \qquad [8]$$

Equations [1], [7], and [8] imply that measurements of attenuation and phase change with depth in soils may be used to yield values of σ_{eff} and T. It should be noted that, if the σ_{eff} is sufficiently high or the f is sufficiently low, that is, $\sigma_{eff}/f \gg 1$, Eq. [1] may be further approximated to yield

$$a = b \simeq 0.0112(\sigma_{eff} f)^{0.5}. \qquad [9]$$

When this approximation is valid, the acoustical data does not give a value for T because T is proportional to $a^2 - b^2$.

Clearly, a soil with surface crusts or with a near-surface compaction zone will not be homogeneous. Nevertheless, if the surface σ_{eff} is sufficiently high, it may appear to be homogeneous in an acoustical-reflection measurement. The simplest alternative would be to model the soil as a double-layer structure (a surface layer over a homogeneous substrate). A more detailed picture of the variation of σ_{eff} and T as a function of d will emerge from probe-microphone data as discussed below.

Sites and Plot Preparation and Nonacoustic Measurements

Description of Soils

The three soil materials used in this study were a washed masonry sand and the surface horizon of two naturally occurring soils: a Grenada silt loam and a Catalpa silty clay loam. The soil material was air dried and sieved through a 6-mm screen. Although the aggregate-size distribution of the Grenada and Catalpa soils were similar, the Catalpa was more granulated and had a more stable structure than the Grenada. This was, in part, due to the higher organic-matter content of the Catalpa soil, which, in combination, with the dominant montmorillonitic clay material, produced a granular structure. The masonry sand consisted primarily of single grains. For convenience, the masonry sand, Grenada silt loam, and Catalpa silty clay loam will be designated as sand, loess, and clay, respectively.

Site Preparation

The 0.3-m-deep soil samples were prepared above the existing soil surface in an open space such that interference from sound reflections of aboveground objects were thought to be negligible. The 3.0 by 6.0 m contiguous test area was subdivided into three plots of 2.0 by 3.0 m each. As shown in Fig. 1c, each plot was partitioned into two equal subplots of 2.0 by 1.5 m. The soil in one subplot was compacted by tamping four incremental soil additions with the 0.29-m face of a 0.04 by 0.29 by 1.20 m wooden board (treatment denoted by "compacted"); the other subplot was loosely packed (treatment denoted by "loosely packed"). Plot border and partitions between plots were made from 0.04 by 0.3 m wooden boards. The plot surfaces were smoothed with a wooden scraper and excess soil was removed so that a table-flat surface condition was obtained. To minimize interference from the abrupt change in surface elevation at the plot border, soil was placed around the plot perimeter so that a gradual transition was obtained between the plot and the surrounding soil surface.

Plot Treatment and Measurements

Acoustic measurements were made following plot preparation on air-dry soil, within 30 min after the application of about 50 mm of rain, and 83 d later on an intermediate soil-wetness condition. The soil plots were covered with a tarp to prevent direct precipitation during the 83 d between wet and dry measurements. For convenience, these soil treatments are denoted as "dry," "wet," and "intermediate," respectively. Rain was applied at an intensity of 50 mm h^{-1} with a multiple-intensity rainfall simulator similar to the one described by Meyer and Harmon (1979). A double layer of 6 by 6 mm window-screen cloth protected the plot surface from the impact of raindrops. However, window screens and soil surface were in direct contact with each other, causing some momentum transfer of the impacting raindrops onto the soil surface. Therefore, raindrop impact may adversely have affected the soil surface structure in this experimental setup.

After each series of acoustic measurements, the plots were sampled in duplicate for soil water content and bulk density. Soil water content determinations were made gravimetrically at 20- to 25-mm depth increments on plots in the wet and intermediate wetness conditions using a 25.4-mm-diam. slotted tube sampler. The sample-retention difficulty of the dry soil required a different sampling technique on the freshly prepared plots. Thin-walled aluminum rings, 76 mm in diameter and either 25.4 or 76 mm long, were carefully inserted in the plots and extracted by excavation. On these samples, both soil-water-content and bulk-density determinations were made. Bulk-density determinations on plots in intermediate wetness conditions were made with 76 by 25.4-mm-diam. rings using the insertion and excavation technique. Bulk-density sampling of the very wet condition was not feasible because of soil softness. Because of the homogeneity of the soil material, the uniformity of the plot-preparation procedures, and the absence of matrix contraction by negative soil water pressure, the best estimate for bulk-density values for this condition is assumed to be the values obtained for the initially dry plots. Table 1 summarizes the measured soil-water-content and bulk-density values for each plot at each series of acoustic measurements. For brevity's sake, data were consolidated where no differences were obtained in the soil water content between successive depth increments. The particle density used to calculate bulk densities was 2.65 g cm^{-3}. The air porosities were determined from the total porosity minus the volumetric water content.

Acoustical Measurements

For each of the soil treatments described above, probe-microphone measurements were made of the pore fluid attenuation and phase constants, and level difference measurements were made of the surface reflection characteristics. These measurements have been extensively described elsewhere (Attenborough et al., 1986; Hess, 1988). Here, we present the ideas and techniques relevant to this particular investigation.

Acoustic Level Difference Measurement

The apparatus for the level difference measurement (Fig. 1a) consisted of a small acoustic point source, two AKG microphones (AKG, Stamford, CT), and the analysis instru-

Table 1. Summary of measured dry bulk density† (ρ_b) and gravimetric water content (θ) as a function of depth (d) for each subplot.

	Sand			Loess			Clay		
	d	ρ_b	θ	d	ρ_b	θ	d	ρ_b	θ
	cm	g cm^{-3}	kg kg^{-1}	cm	g cm^{-3}	kg kg^{-1}	cm	g cm^{-3}	kg kg^{-1}
				Dry soil					
Compacted	0–10	1.54	0.01	0–10	1.12	0.06	0–10	1.16	0.09
Loosely packed	0–10	1.39	0.03	0–10	1.09	0.06	0–10	1.17	0.09
				Wet soil					
Compacted	0–2	1.54	0.04	0–10	1.12	0.28	0–18	1.16	0.25
	2–8	1.54	0.05	10–14	1.12	0.27	18–26	1.16	0.24
	8–10	1.54	0.07						
	10–12	1.54	0.09	14–20	1.12	0.26			
	12–14	1.54	0.11	20–26	1.12	0.24			
	14–16	1.54	0.13						
Loosely packed	0–6	1.39	0.05	0–12	1.09	0.28	0–26	1.17	0.28
	6–8	1.39	0.06	12–18	1.09	0.27			
	8–14	1.39	0.08	18–26	1.09	0.24			
	14–16	1.39	0.12						
				Intermediate soil‡					
Compacted	0–8	1.55	0.01	0–2	1.14	0.16	0–2	1.24	0.18
	8–10	1.55	0.02	2–6	1.14	0.18	2–6	1.24	0.22
	10–18	1.55	0.03	6–8	1.14	0.19	6–18	1.24	0.24
				8–20	1.14	0.20			

† Bulk density was assumed to be uniform for the plot depth because of uniformity in soil material and plot preparation.

‡ The loosely packed plots in an intermediate soil wetness condition were inadvertently not sampled for water content and bulk density. Instead, the corresponding values for the compacted plots were used in the analysis.

mentation. The acoustic point source was constructed by connecting a Peavey compressional driver (Model 22A, Peavey Electronics Corp., Meridian, MS) to a 0.025-m i.d., 30-cm-long brass pipe. The source was mounted to a rod and tripod stand with heavy-duty test-tube-type clamps. The AKG microphones were mounted to a similar stand in such a way that the source and receivers were all in a vertical plane (Fig. 1a). The level difference apparatus was set up over each subplot such that the point of specular reflection was at the center of the subplot. The lower microphone was always positioned 10 cm above the soil surface. The position of the upper microphone was varied from 30 to 50 cm, as different geometries are required in the data-analysis procedure. The horizontal separation between source and microphones was recorded.

Before measurements and several times during the course of the measurements, calibration tones were recorded on the microphones. The calibration signals, 104 dB at 1 kHz and 114 dB at 1 kHz, were approximately the same as the source level at the microphones.

The acoustic point source emitted white noise over the frequency range 100 Hz to 10 kHz. A Fourier transform was carried out on the signals from both microphones using a Fast Fourier Transform (FFT) analyzer. The analyzer was used to calculate, in dB, the transfer function representing the output of the lower microphone subtracted from the output of the upper microphone as a function of f. Thus, the measurement is termed acoustic level difference or simply level difference. The level difference was computed from the average of 32 transfer-function measurements. Once the measurement at one geometry was complete, the source height and upper microphone height were changed and recorded. The separation distance between the source and microphone was also determined again. This procedure was carried out over each of the subplots for the wet, dry, and intermediate soil-water conditions.

The electrical signals from the microphones were amplified with Tektronix AM502 differential amplifiers (Tektronix, Huntsville, AL) and then analyzed with a Hewlett Packard Model 3562 FFT analyzer (Hewlett Packard Co., Nashville, TN). Data from the analyzer could be stored on disk or transferred to a Masscomp 5550 computer (Concurrent Computer Corp., Westford, MA) via an IEEE-488 interface for further analysis.

Probe-Microphone Measurements

The experimental setup for measurements of sound beneath the soil surface consists of a loudspeaker system, probe microphone, reference microphone, and the associated instrumentation to record and analyze the acoustic signals received by the microphone.

The loudspeaker system consists of four independent vented boxes, each of which has an internal volume of 725 L and is tuned to 20 Hz with ports. On the front face of each box is mounted a modified Peavey 46-cm driver. Typ-

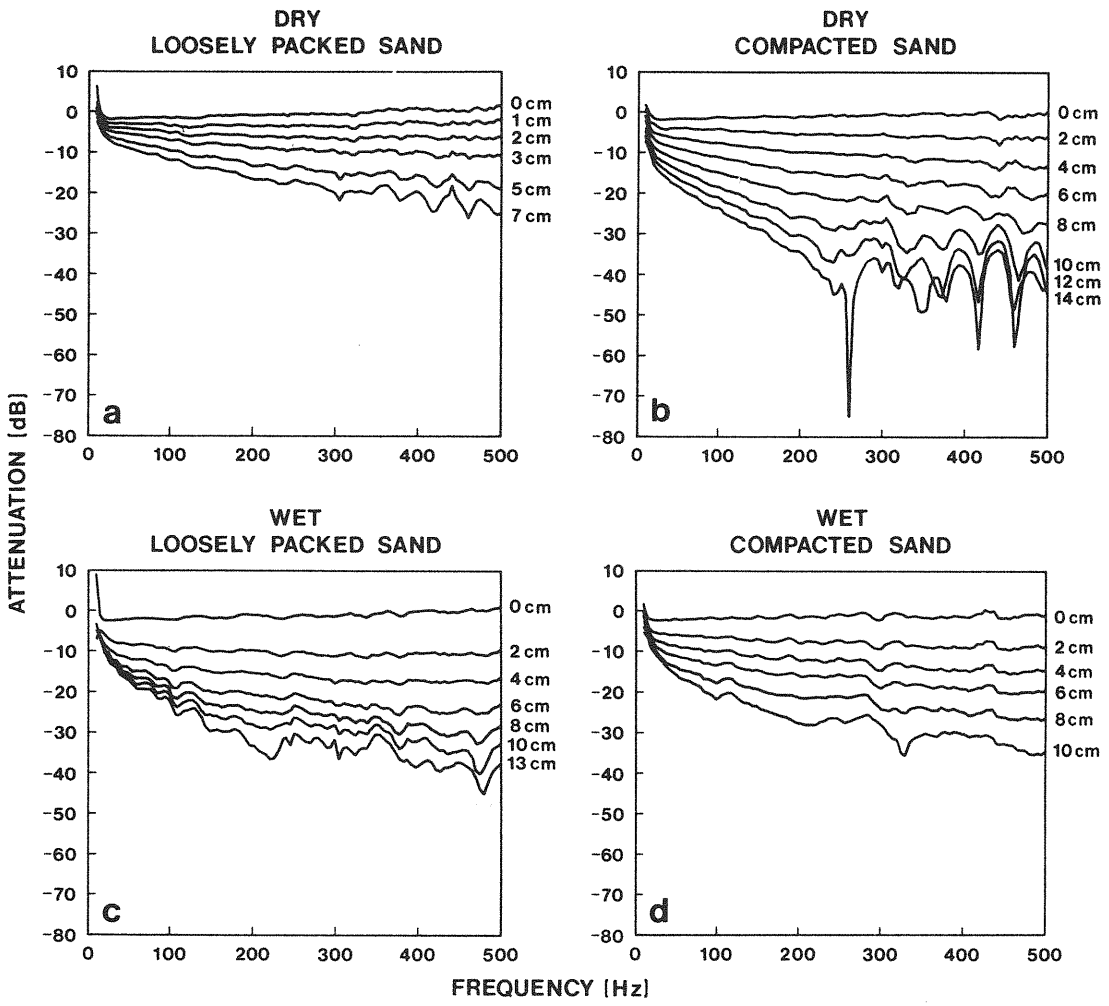

Fig. 3. Probe-microphone data obtained in a) dry, loosely packed sand; b) dry, compacted sand; c) wet, loosely packed sand; and d) wet, compacted sand. Numbers on the right side of each graph refer to the probe-microphone depth below the surface in cm.

ically, off-the-shelf speakers are not capable of producing sound levels sufficient to make the probe-microphone measurements in most soils. The reference microphone was an AKG model C460B, which has a flat frequency response from 20 Hz to 20 kHz. This microphone was used because its low frequency roll-off reduces the effect of wind noise. A second AKG microphone was inserted into a specially designed brass tube with a nose cone that allows the microphone element to sense the pore fluid pressure in the soil. The design and use of this type of microphone has been described elsewhere (Attenborough et al., 1986; Attenborough and Hess, 1985).

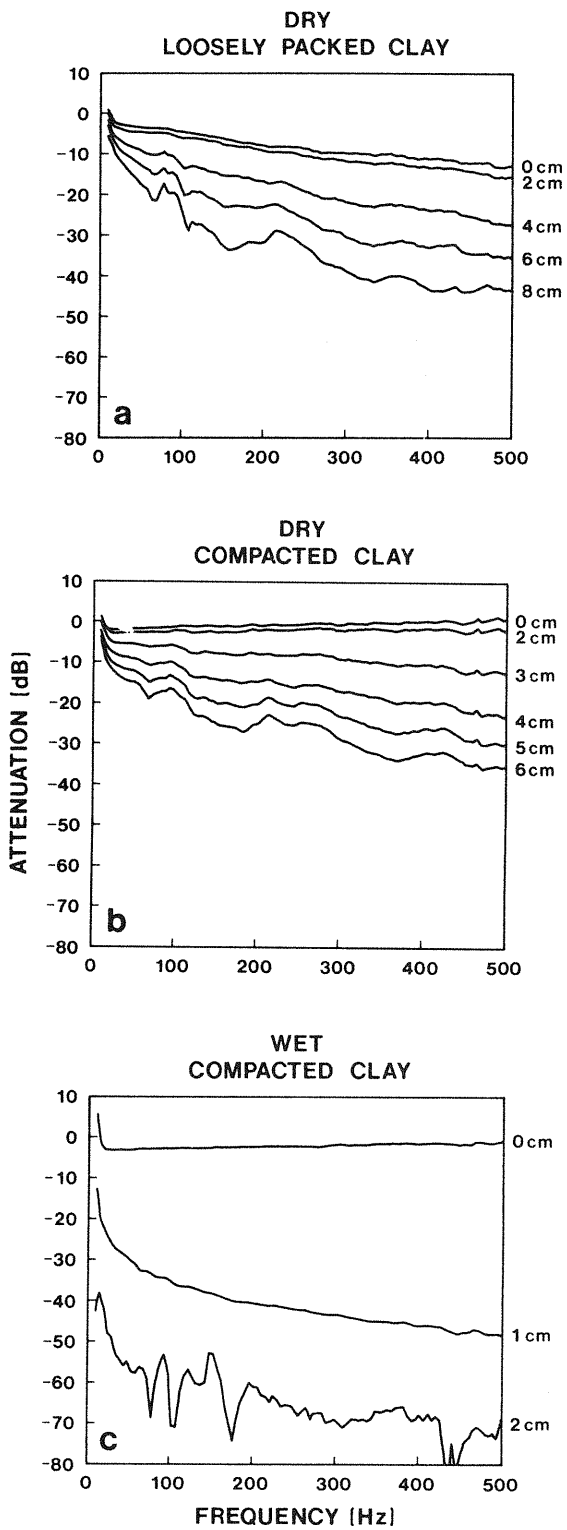

Fig. 4. Probe-microphone data obtained in a) dry, loosely packed clay; b) dry, compacted clay; and c) wet, compacted clay. Numbers on the right side of each graph refer to the probe-microphone depth below the surface in cm.

The procedure for measurement of the pore-fluid wave speed and attenuation is as follows. The probe and reference microphones were co-located (Fig. 1b) at the approximate center of one of the soil treatments with the probe microphone supported in the vertical position. Such locations are indicated in Fig. 1d. The loudspeaker system, positioned on a small truck, was 10 m from the test plots and was driven by a sinusoidal source. The source frequency was varied linearly from 20 to 500 Hz at steps of approximately 1 Hz. The amplitude and phase of the signals received by the probe and reference microphones were measured with both microphones on the surface. The magnitude and phase of the transfer function between the probe and reference microphones, defined as the probe-microphone output divided by the reference-microphone output, was displayed on the monitor screen of the FFT analyzer and stored on disk for later analysis. Then the probe was pushed some specified distance below the soil surface and the measurement of the transfer function was repeated. This procedure was repeated for increasing depths of the probe until the probe signal decreased to the background noise level.

Ideally, the transfer function between two co-located identical microphones would be unity (0 dB). For example, see the 0-cm line of Fig. 3a. Because the probe-microphone frequency response is different from that of the reference microphone, the 0-cm curve is not 0 dB over the entire frequency range. However, when the attenuation between two depths is determined, these effects cancel. It should be noted that, in Fig. 4a, the 0-cm line is different from all the other probe-microphone figures. This is due to a peculiar filter setting for one of the microphone signal amplifiers. Since only differences in attenuation as a function of depth are important, the effect cancels for this measurement.

By comparing the difference in the magnitude of the transfer function for each depth interval, say 1 cm and 2 cm, the pore fluid sound attenuation (the left side of Eq. [7]) is determined between these two depths as the difference in transfer function values in dB at each frequency point. Similarly, knowledge of the phase of the transfer function at two depths allows the phase speed to be determined from use of Eq. [8] over the particular depth range as a function of frequency.

Care was taken that no air leaks existed at the point of entry of the probe microphone into the soil. Air leaks result in significantly less attenuation than that representative of the soil treatment. Special techniques have been developed for preventing and sealing air leaks. In the dry prepared plots of this study, however, air-leak problems were minimal. A small paint brush was used to move enough soil to fill any cracks that might have developed in the probe entry area. These cracks are typically less than 1 mm in width. In measurements the wet loess and clay soils, the sealing technique was different. In these soils under the wet conditions, the process of inserting the probe not only caused leaks at the entry point of the soil surface but also caused the air holes in the probe's nose cone to seal. The latter was noticed on inspection after the probe was removed from the plot following completion of the measurements. Consequently, for some runs, the data had to be rejected because of sealing of the probe's air holes. The surface leaks were sealed by using a small blade an a highly viscous fluid. The fluid used was commercially available STP Oil Treatment. For the plots with intermediate soil water conditions, a small hole was

drilled with a diameter somewhat smaller than the probe. The probe was then inserted into the hole to the desired depth and the same technique that was described for the wet soils was used to seal the entry.

RESULTS AND DISCUSSION

Qualitative Interpretation Of Acoustical Data

Sound Level Difference Data

As long as the soil is homogeneous to several centimeters depth, the physical principles discussed above, together with Fig. 2a, enable straightforward qualitative interpretation of level difference spectra. Figure 2b shows level difference spectra obtained with similar geometries over the loosely packed sand at an intermediate soil water content, and over the compacted, wet clay. The first minimum in the level difference spectrum above the wet, compacted clay is at a higher frequency than that in the spectrum obtained over the intermediate, loosely packed sand. From the discussion of Fig. 2a above, this implies that the wet, compacted clay must have a higher σ_{eff} than the intermediate, loosely packed sand. In contrast, the level difference spectra shown in Fig. 2c obtained over wet, loosely packed loess and wet, loosely packed clay indicates similar σ_{eff}. On the other hand, spectra in Fig. 2d obtained over dry, loosely packed sand and dry, loosely packed clay indicate differences in the type of acoustic response of these two soil media. In this case, the level difference spectra have first dips at the same frequency but are of distinctly different form, suggesting that these soils have different acoustical (physical) properties. This suggests, for example, that the clay has a near-surface structure/porosity that is different from relatively uniform sand.

Probe-Microphone Data

As indicated previously, soils with a large air flow resistivity will result in a large sound attenuation and phase change at a given f and probe-microphone depth (d). Hence, it should be possible qualitatively to explore differences in acoustic transmission data obtained in different soils and for different conditions of a given soil. It is important, however, to explain first the physical significance of the dB unit of attenuation. A 6-dB decrease in sound pressure level represents a halving of the acoustic pressure. Consequently, for a soil in which the measured attenuation is 6 dB cm^{-1} at a given f, the pressure of penetrating sound at that f will be halved with every centimeter traveled. Other values of attenuation may be judged against this information.

It should be noted that the depth to which the probe can be used to make reliable measurements will depend on the sound level at the source. As the probe is pushed deeper in the soil, the attenuation reduces the signal, eventually to the acoustic background, and the transfer function becomes suspect (see, for example, the 14-cm curve in Fig. 3b for $f > 200$ Hz).

Sound attenuation for dry, loosely packed soils. The change in attenuation with d as measured by the probe-microphone data in sand (Fig. 3a) is rather uniform and is 4 dB cm^{-1} at 500 Hz. The attenuation per centimeter between 0 and 1 cm or 2 and 3 cm at any particular f is approximately the same for the two ranges. The same observation can also be made for the other d ranges in this figure with the exception of 5 to 7 cm between 350 and 500 Hz. This structure in the attenuation for this range is due to the low sound level at the probe microphone at these d and f. However, the data below 350 Hz for this d is still indicating that the sand is homogeneous in the 5 to 7-cm range. The uniform change with d indicates that the sand is homogeneous to 7 cm. None of the other two soils reveal this uniformity over the first few centimeters (Fig. 4a for clay, Fig. 5a for loess). Indeed, both clay and loess appear to have thin, relatively low σ_{eff} layers below the surface, the σ_{eff} of these thin surface layers being less than that of the sand. Below these thin layers, both clay and loess appear to have more attenuation, implying high σ_{eff} in their dry, loosely packed state. The loess soil is fairly uniform between 1 and 3 cm below the surface. The clay has a layer of slightly higher σ_{eff} between 2 and 4 cm and is uniform between the 4- and 8-cm depth.

Effects of compaction. Down to the 8-cm depth, compaction appears to reduce slightly the attenuation of sound in the sand (compare Fig. 3a and b) from about 4 dB cm^{-1} to 3 dB cm^{-1} at 500 Hz. This appears to imply that the σ_{eff} of the sand is slightly reduced by packing. However, the effect is not large and is within the reproducibility range of the probe measurements. On the other hand, the relatively high attenuation in the layer between 2- to 4-cm depth in the loosely packed clay is appreciably increased by compaction (compare Fig. 4a and b). This suggests an increase in σ_{eff} at this d as a result of packing the clay soil. At 500 Hz, the layer between 2- and 4-cm depth has an attenuation rate of 10 dB cm^{-1} after compaction (Fig. 4b). On the other hand, the attenuation (and hence, σ_{eff}) between 4- and 6-cm depths is relatively unaffected by packing (Fig. 4b) and only increases slightly from 4 to 6 dB cm^{-1} at 500 Hz. In loess, both the thin surface layer with relatively low attenuation and the 1- to 2-cm depth layers are strongly affected by packing (compare Fig. 5a and b). Because of the high attenuation in both dry loess states, a comparison below 2 cm is prohibited.

Effects of wetting of loosely packed soil. The sound attenuations with d measured by the probe microphone in loosely packed sand are not greatly changed by wetting (Fig. 3a and c). The attenuation in wet sand is approximately 4 dB cm^{-1} at 500 Hz. Because of the rapid drainage of applied water to deeper parts of the profile, the σ_{eff} is unchanged by wetting and subsequent drying. On the other hand, the probe microphone reveals that wetting has a considerable effect on the near-surface properties of the loosely packed loess soil (compare Fig. 5a and c). No probe data were obtained in the wet, loosely packed clay or loess.

Effects of compaction and wetting. On the clay soil, the wet, compacted condition results in sound attenuation of nearly 45 dB at 500 Hz over the 1st cm (Fig. 4c). This represents 40 dB more attenuation for the 1st cm at 500 Hz than in the dry, compacted condition

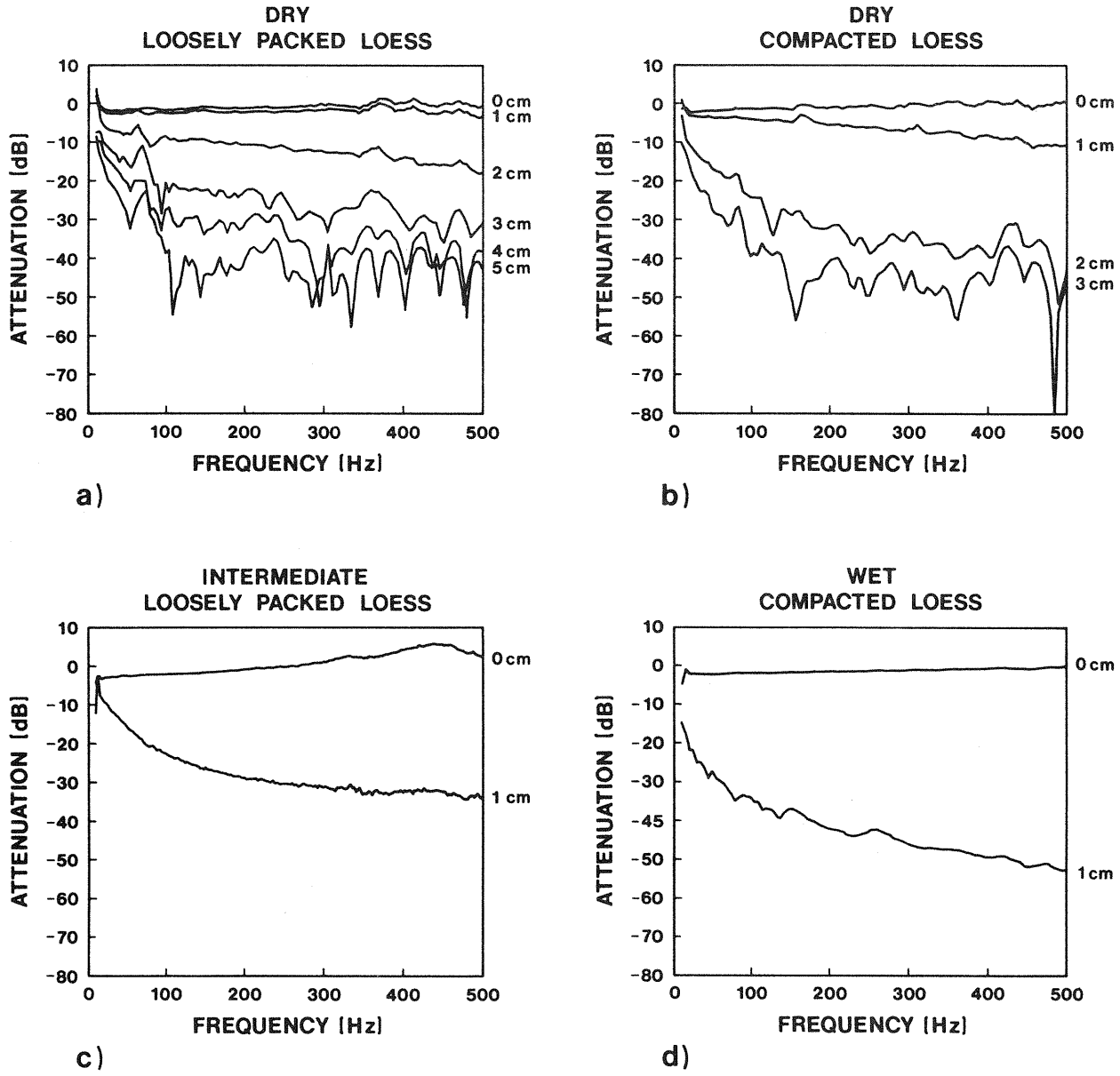

Fig. 5. Probe-microphone data obtained in a) dry, loosely packed loess; b) dry, compacted loess; c) intermediate, loosely packed loess; and d) wet, compacted loess. Numbers on the right side of each graph refer to the probe-microphone depth below the surface in cm.

(Fig. 4b). Although the results for the 2nd-cm depth in the wet, compacted state are less reliable because appreciable attenuation that took place in the 1st-cm layer, the data suggest an increased σ_{eff}, compared with that obtained for the dry, compacted soil.

A similarly marked effect due to wetting and packing is observed with the probe data obtained in loess (Fig. 5d). The attenuation in dB cm^{-1} over the 1st cm in the wet, compacted state is much larger than that measured in the dry, compacted condition (compare Fig. 5b and d).

The effect of wetting on compacted sand, as shown by the probe data (compare Fig. 3b and d) is to increase the attenuation over the first 2 cm to a value that is greater than that for the corresponding depth of the dry, compacted condition.

Quantitative Interpretation Of Acoustical Data: Deduction Of Soil Physical Parameters

Fitting Algorithms

The process of obtaining quantitative information from measured acoustic level difference spectra and probe-microphone spectra involves comparison with theoretical predictions. If the soil is homogeneous to a depth of several centimeters, then the measured level difference should conform to that predicted by Eq. [2] through [4] and Eq. [A7] with appropriate values for Ω, σ_{eff}, and T. Level difference spectra obtained from two source-receiver geometries are necessary to enable an unambiguous choice of sets of parameter values that satisfy both spectra. In this study, a numerical least-squares fitting routine is used to deter-

Table 2. Best-fit parameters† obtained from level difference data over masonry sand using geometries listed in Table 3.

Condition	Geometry	σ_{eff}, 10^3 N s m^{-4}	T	Ω	RMS fitting error	Measured Ω
Dry,	1	17	3.4	0.41‡	1.8	0.45
loosely	1	11	2.1	0.33	1.8	
packed	2	12	2.1	0.43‡	2.8	0.45
	2	26	4.5	0.63	2.8	
Dry,						
compacted	1	39	4.7	0.53	2.0	
	1	23	2.9	0.41‡	2.0	0.41
	2	16	2.1	0.43‡	2.8	
	2	35	4.5	0.62	2.8	
Intermediate,						
compacted	1	27	2.4	0.41	1.3	0.37
Intermediate,	1	6.1	1.4	0.41	4.0	0.46
loosely	1	5.9	1.3	0.35	4.0	
packed	2	6.2	1.6	0.39	2.7	

† σ_{eff} = effective flow resistivity; T = tortuosity; Ω = porosity of air-filled connected pores; measured Ω = total porosity minus volumetric water content; RMS fitting error = square root of the sum of squared errors for the best-fit parameter set.
‡ Parameter sets with the most consistent values of Ω and σ_{eff} for the two geometries.

Table 3. Geometries used in level difference measurements. Geometry 1 has both H and h_2 equal to 0.3 m. Geometry 2 has both H and h_2 equal to 0.4 m. Distance h_1 = 0.1 m in all cases. (See Fig. 1a for parameters.)

Soil	Condition	Geometry	S, m
Loess	Dry, compacted	1	1.58
		2	1.58
Sand	Dry, compacted	1	1.59
		2	1.61
	Dry, loosely packed	1	1.57
		2	1.57
Clay	Dry, compacted	1	1.66
		2	1.66
	Dry, loosely packed	1	1.61
		2	1.63
Loess	Intermediate, loosely packed	1	1.40
		2	1.40
Clay	Intermediate, compacted	1	1.40
		2	1.40
	Intermediate, loosely packed	1	1.40
		2	1.40
Sand	Intermediate, compacted	1	1.40
		2	1.40
	Intermediate, loosely packed	1	1.40
		2	1.40
Loess	Wet, compacted	2	1.59
Clay	Wet, compacted	1	1.62
		2	1.62

mine the best-fit values of Ω, σ_{eff}, and T. The routine calculates the sum of the squared differences between theoretical prediction and measured acoustical data at all of the data frequencies. Then the routine attempts to minimize this sum by varying the soil parameters. Several of the two level difference spectra (i.e., two source-receiver geometries) for each soil and soil condition have parameter sets corresponding to local minima in the squared-error sum. The subsequent choice of best-fit parameters uses equivalence of Ω values determined from each source height as the main criterion. The square root of the sum of squared errors for the best-fit parameter set, henceforth called the RMS error, is then an indication of the relative goodness of fit and, therefore, of the reliability of the result. An RMS error of zero would be ideal.

Although, in principle, a similar fitting procedure for the relative phase and attenuation measured by the probe microphone is possible, a less rigorous procedure has been adopted here. For a given f, the real and imaginary parts of Eq. [1] are functions of σ_{eff} and T. Consequently, values of a and b deduced from probe-microphone measurements may be used through Eq. [7] and [8] to give simultaneous equations that, in turn, may be solved for σ_{eff} and T. This procedure has been followed with probe-microphone data obtained in sand and in the first 2 cm of the relatively low σ_{eff} soils. Values of σ_{eff} and T have been calculated at every data frequency up to 500 Hz and the results have been averaged. For the other soils and depths, the σ_{eff} were sufficiently high that, below the highest f of the measurement (500 Hz), the approximation given by Eq. [9] was valid. This approximation implies that a and b are nearly equal and, for a given f, are determined entirely by the value of σ_{eff}. Consequently, attempts to fit σ_{eff} and T give arbitrary and unlikely values for T. Nevertheless, in the majority of these cases, the values of σ_{eff} at every f yielded by Eq. [7] and [8] have been averaged. Note that, according to Eq. [7] and [8], b should always be $\leq a$. In a few cases, the values of b calculated from the data were greater than those calculated for a at many data frequencies. In these few cases, Eq. [9] was used to yield a value for σ_{eff} at the lowest data frequency consistent with equal values of a and b. The single f used for all of these values, except for the dry compacted clay (4–6 cm) and dry compacted loess (1–2 cm) was 150 Hz. For these soils at these d, the single f used was 300 and 200 Hz, respectively.

Results of Analyses of Level Difference Data

Sand. Table 2 shows best-fit parameters obtained from level difference data over sand using the geometries listed in Table 3. The lines marked with ‡ for dry, loosely packed and dry, compacted sand indicate those parameter sets in which the most consistent values of Ω and σ_{eff} have been obtained. As an example of parameter-choice criteria, consider dry, loosely packed sand. For Geometry 1, the best fit to the data yielded two local minima of the RMS error, with Ω of 0.41 and 0.33, and with an RMS error of 1.8. For Geometry 2, the local minima of the RMS error gave Ω of 0.43 and 0.63, with an RMS error of 2.8. Thus, in this case, the best-fit Ω value would be the average of the two closest values, 0.42. Comparisons between measured and predicted level difference spectra are shown in Fig. 6a and b. The values of σ_{eff}, T, and Ω on the lines marked with ‡ in Table 2 have been chosen as the acoustically deduced values. The results suggest very little change in the air-filled porosity of the sand with packing. Moreover, the values are within 8% of those measured by nonacoustic means.

Clay. Table 4 shows best-fit parameters obtained from level difference data over the clay soil using the geometries listed in Table 3. An example fit is shown in Fig. 6c for dry, compacted clay. Only the consistent best-fit parameters are shown in Table 4. Acoustically, the surface of the loosely packed clay appears to have

Table 4. Best-fit parameters† obtained from level difference data over Catalpa silty clay loam using geometries listed in Table 3.

Condition	Geometry	σ_{eff}, 10^3 N s m^{-4}	T	Ω	RMS fitting error	Measured Ω
Dry, loosely packed	1	37	1.6	0.40	1.5	0.45
	2	43	1.8	0.41	1.5	0.45
Dry, compacted	1	35	4.7	0.41	1.5	0.45
	2	43	2.3	0.42	1.3	0.45
Wet, compacted	1	160	12.7	0.24	3.0	0.28
	2	100	16.5	0.25	3.7	
Intermediate, compacted	1	3.9	2.5	0.31	2.1	0.26
	2	3.2	2.1	0.28	2.1	
Intermediate, loosely packed	1	5.6	2.9	0.40	2.6	
	2	5.1	2.9	0.40	2.9	

† σ_{eff} = effective flow resistivity; T = tortuosity; Ω = porosity of air-filled connected pores; measured Ω = total porosity minus volumetric water content; RMS fitting error = square root of the sum of squared errors for the best-fit parameter set.

a similar Ω to that of the compacted clay. This is supported by the nonacoustic measurements, which indicate identical Ω for the dry, loosely packed and compacted clay soil. The reduction in Ω near the surface of compacted clay from 0.45 to 0.28 as a result of wetting, which is indicated by the conventional data, is fairly accurately predicted from the acoustical data. However, the acoustically deduced Ω for the loosely packed and dry, compacted clay are somewhat smaller by approximately 10% than those obtained from conventional measurements.

A remarkable feature of the parameters deduced from level difference measurements is the apparent low σ_{eff} of the compacted and loosely packed clay for the intermediate soil moisture condition. This effect is not observable in the probe-microphone data and is probably due to surface cracks that were present on

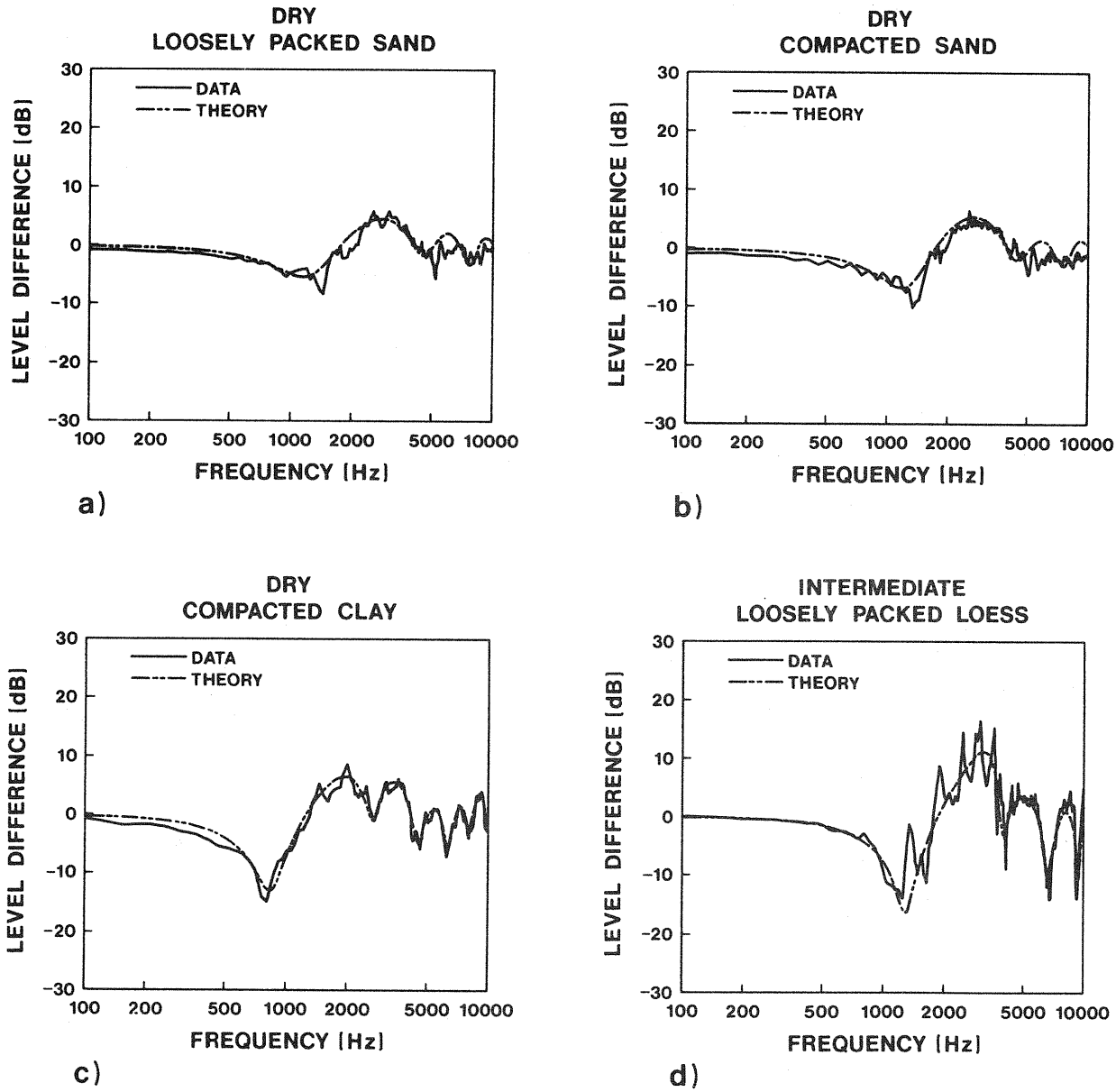

Fig. 6. Measured and predicted level difference spectra over a) dry, loosely packed sand; b) dry, compacted sand; c) dry, compacted clay; and d) intermediate, loosely packed loess.

the clay surface. In contrast, care was taken to avoid areas with clear surface cracks when probe-microphone-measurement locations were selected.

Loess. Results obtained by fitting the homogeneous model to level difference data obtained over loess in its dry, compacted and intermediate, loosely packed states are shown in Table 5 based on the measurement geometries listed in Table 3. For these high σ_{eff} surfaces, the fits to measurements at all geometries give Ω within 5% of the conventionally measured values. An example of a fit to a level difference spectrum obtained over loess soil is shown in Fig. 6d. The acoustical technique distinguishes between the Ω of the dry, compacted and intermediate, loosely packed states in a way that agrees with data obtained with the conventional technique. It has not been possible to obtain fits to the level difference data above dry, loosely packed loess using the homogeneous model due, perhaps, to layering of the soil. The acoustical technique gives Ω for loess in a wet, compacted state that are within 20% of those obtained conventionally.

Table 5. Best-fit parameters obtained from level difference data over Grenada silt loam loess using geometries listed in Table 3.

Condition	Geometry	σ_{eff}, 10^3 N s m^{-4}	T	Ω	RMS fitting error	Measured Ω
Dry,	1	200	12.1	0.46	2.3	0.49
compacted	1	190	11.2	0.44	2.3	0.49
	2	180	9.5	0.47	2.3	0.49
Intermediate,	1	150	2.0	0.36	3.1	0.37
loosely	1	170	2.3	0.38	3.1	0.37
packed	2	78	10.0	0.37	3.2	0.37
Wet,	2	90	17.2	0.24	3.7	0.27
compacted	2	72	13.7	0.21	3.7	

† σ_{eff} = effective flow resistivity; T = tortuosity; Ω = porosity of air-filled connected pores; measured Ω = total porosity minus volumetric water content; RMS fitting error = square root of the sum of squared errors for the best-fit parameter set.

Results of Analysis of Probe-Microphone Data

Sand. Table 6 shows the quantitative results from analysis of probe-microphone data obtained in sand for all combinations of packing and wetness. The relatively low σ_{eff} of the sand means that values of a and b obtained from the data below 500 Hz are marginally different. Thus, as argued above, the analysis was able to yield values for both σ_{eff} and T. On the other hand, the closeness of the a and b values means that the deduced T values are not very reliable and indeed, in some cases, could not be determined. In such cases, the σ_{eff} has been deduced from the value for b at 400 Hz using Eq. [9]. More precise determinations would follow from data obtained at higher f (Hess, 1988). Multiple values for a given d represent results of fitting probe measurements made at different locations on a given soil condition.

An example of fitting the measured k is shown in Fig. 7a. For dry and wet, loosely packed sand conditions, the probe data indicate consistently lower σ_{eff} below 3-cm depth than in the first 3 cm (see Table 6). On the other hand, the σ_{eff} obtained in dry, compacted and intermediate, compacted conditions are relatively uniform with depth.

Clay. Table 7 presents values of σ_{eff} and T data deduced from probe data obtained for four combinations of wetness and packing of the clay soil. No probe data were obtained for the wet, loosely packed and intermediate, loosely packed states. An example of fitting is shown in Fig. 7b. The relatively poor fit to the data, and, in particular, the frequency dependence may indicate lack of vertical homogeneity between the soil surface and 2-cm depth. Again, below 1-cm depth in the dry, loosely packed case and at all d for all other cases, the high σ_{eff} and the restricted f range of the data either precluded deduction of T or made the deduction of T values unreliable. Nevertheless, there is a

Table 6. Results from analyses of probe microphone data obtained in masonry sand for six different conditions.

	Soil Condition											
	Dry, loosely packed		Dry, compacted		Wet, loosely packed		Wet, compacted		Intermediate, loosely packed		Intermediate, compacted	
Depth, cm	σ_{eff}†	T‡	σ_{eff}	T	σ_{eff}	T	σ_{eff}	T	σ_{eff}	T	σ_{eff}	T
0–1	40	16							37	30		
0–2			26	6	120§		18				20	15
							5.5§					
1–2	37	8							30	14		
2–3	41	7							15	6		
2–4			25	3	46§		32				14	3
							30§					
3–4									7	2		
3–5	24	9										
4–5									18	3		
4–6			27	3	34	10	16	2			16	1
							15	1				
5–6									9	1		
5–7	17	5										
6–7									15	1		
6–8			26	7	15	10	17	1			19	2
							22	5				
7–8									16	1		
8–10					11	10						
7–11	11	4										
10–13					8.5	13						

† σ_{eff} = effective flow resistivity, measured in units of 10^3 N s m^{-4}.
‡ T = tortuosity.
§ A different fitting procedure was used for these data.

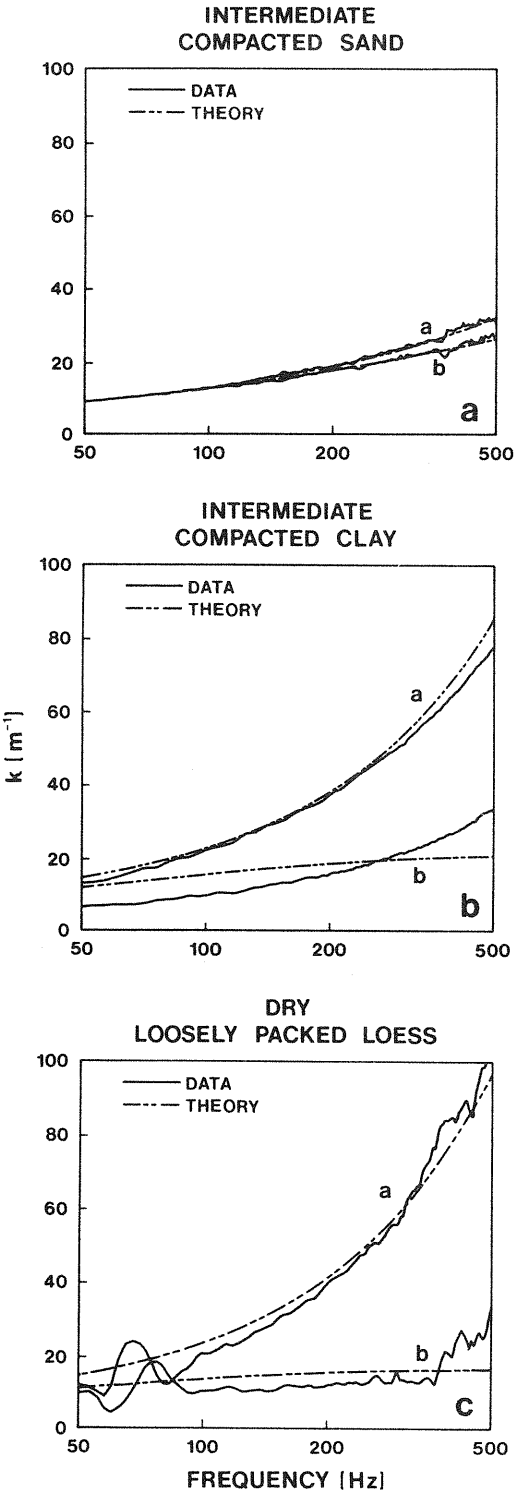

Fig. 7. Measured and predicted propagation constant a) between 2 and 4 cm in intermediate, compacted sand (the relationships between real and imaginary parts of the propagation constant and the measured attenuations and phase changes have been assumed to be given by Eq. [7] and [8]); b) between 0- and 2-cm depth in intermediate, compacted clay; and c) between 0- and 1-cm depth in dry, loosely packed loess.

noticeable trend for the acoustically deduced T values to increase with d in the dry, loosely packed condition. The σ_{eff} between 2 and 4 cm in the dry, compacted case is found to be several times those obtained above or below this zone. Compaction increases the σ_{eff} between the surface and 2-cm depth, and wetting subsequently increases it further.

Table 7. Results from analyses of probe-microphone data obtained in Catalpa silty clay loam for four different conditions.

Depth, cm	Soil Condition: Dry, loosely packed σ_{eff}†	T‡	Dry, compacted σ_{eff}	T	Wet, compacted σ_{eff}	T	Intermediate, compacted σ_{eff}	T
0–1					9100§		62	130
					8800§			
0–2	8	5	160	140			29	55
	6	8	13	52				
1–2					1300		61	43
1–3					1700			
2–3							100	23
							36	28
2–4	110		190					
	91	11	190	62				
3–4							64	37
3–5							41	31
4–5							20	4
4–6	28	30	70	1				
	57	26	120§					
5–6							5307	12.6
6–8	95	78	50	16				

† σ_{eff} = effective flow resistivity, measured in units of 10^3 N s m^{-4}.
‡ T = tortuosity.
§ A different fitting procedure was used for these data.

Loess. Quantitative results from probe data in loess are shown in Table 8 for four out of the six possible combinations of wetness and compaction. No data were taken in the remaining two states. An example of fitting is shown in Fig. 7c. With the exception of the 1st cm in the dry, loosely packed case, these data show uniformly high σ_{eff} and, again, for reasons explained above, the T values are either unreliable or unobtainable. Compaction increases the σ_{eff} of the dry, loosely packed case several times. Subsequent wetting produces results that vary with probe location but suggest a further increase in σ_{eff}.

Comparison of Parameters Deduced from Probe and Level Difference Spectra

While the σ_{eff} and T of the sand for most conditions deduced by either probe-microphone or level-difference techniques are of the same order, large differences are found between the respective quantitative deductions for the other soils. This may be the consequence of the small area size being sampled by the probe relative to that involved in level-difference measurements. Probe-microphone measurements are taken below the soil surface, whereas level difference measurements are most sensitive to the soil-surface condition. The σ_{eff} deduced from level difference data by assuming homogeneity may also be in error when applied to soils clearly shown to be heterogeneous by probe measurements. Despite the absolute discrepancies, the probe values generally indicate the same type of change with changing soil conditions as do the level difference values.

CONCLUSIONS

An acoustical-reflection technique has been shown to enable deduction of Ω noninvasively, typically to within 10% of conventionally obtained values for three different soils and several different soil condi-

Table 8. Results of analyses of probe-microphone data obtained in Grenada silt loam loess for four different conditions.

Depth, cm	Soil Condition: Dry, loosely packed		Dry, compacted		Wet, compacted		Intermediate, loosely packed	
	σ_{eff}†	T‡	σ_{eff}	T	σ_{eff}	T	σ_{eff}	T
0–1	26	70	250	320	8800§		1300	1800
	92	168	230	190			1900	1100
1–2	390	270	3600§					
	1700	1100	3200					
2–3	780	2000	2100					
	1700	5700	3000					
3–4	560	1100						
	130	650						

† σ_{eff} = effective flow resistivity, measured in units of 10^3 N s m^{-4}.
‡ T = tortuosity.
§ A different fitting procedure was used for these data.

tions. Where large differences occurred, such as for dry, compacted clay, they may be attributed to the shallow sampling depth of the acoustic-reflection technique, compared with gravimetric sampling (>3 cm). Errors in the gravimetric-sampling technique are also possible.

It should also be mentioned that the acoustic measurements were not made under ideal conditions. The test-plot surface was 30 cm above the surrounding soil, thus possibly causing edge diffraction that can contribute to the level difference signals. Two of the subplots were less than 2 m from a wooden building, which may have been responsible for spurious reflections. Experimental level difference measurements closely resembling the ideal computed level difference curves in Fig. 2a may be obtained over flat unobstructed sites (Hess, 1988).

An acoustic probe-microphone technique has been shown to indicate the variation of soil conditions with depth over the first few centimeters for several different soil treatments. In particular, the probe technique indicates permeable surface layers in clay in the dry, loosely packed state, and the formation of a compaction pan. This technique also shows a decrease in surface permeability after packing and wetting in both clay and loess soils.

Although the probe technique is invasive, essentially it samples an area of soil that is relatively undisturbed and outside the probe rather than the enclosed disturbed volumes involved in other invasive techniques. It has been shown elsewhere (Van der Haarst and Stakman, 1965) that data obtained to a higher f than those reported here enables the accurate deduction of T. Furthermore, assuming the validity of the Bruggeman relationship, $T = \Omega^{-n'}$ (Attenborough, 1983), where n' is a grain-shape factor, and assuming that the grain-shape factor does not vary with d, it is possible to use the probe data to deduce variation of Ω with d.

It should be mentioned also that data obtained above heterogeneous soils has been fitted successfully elsewhere (Hess, 1988) using a double-layer model with corresponding improvements in the predictions of surface Ω and permeability.

ACKNOWLEDGMENTS

This work was supported in part by the USDA. We acknowledge the support of the Agriculture and Food Research Council, UK and the Dep.of Physics and Astronomy, University of Mississippi. We also acknowledge the support of the National Center for Physical Acoustics. We are grateful to Mr. David Craig and Mr. Heui-Seol Roh for their assistance in data collection.

APPENDIX

The Computation of Level Difference Spectra

In Fig. 1a, a point source and two receivers are located above a flat rigid surface. The total pressure (P_{tot}) received at either microphone is composed of a direct (r_1) and a reflected (r_2) sound ray. This may be expressed mathematically as

$$P_{tot} = \frac{\exp(ik_0 r_1)}{r_1} + Q\frac{\exp(ik_0 r_2)}{r_2} \qquad [A1]$$

where k_0 is the propagation constant (Kinsler et al., 1980) of sound in air. In Eq. [A1], r_1 is the source-to-microphone distance and r_2 is the source-to-ground-to-microphone distance. The reflection coefficient, Q, is given by Eq. [3] and [4] and is dependent on the angle of incidence (ψ) of the sound ray to the vertical on a homogeneous soil, the impedance of the soil (Z) and the frequency (f). Equation [4] can be rewritten in greater detail (Chien and Soroka, 1980) as

$$Q = R + (1 - R)F(f,\psi,Z) \qquad [A2]$$

where $F(f,\psi,Z)$ is called the boundary loss factor and is given by

$$F(f,\psi,Z) = 1 + i\sqrt{\pi}\,\omega \exp(\omega^2)\,\mathrm{erfc}(i\omega) \qquad [A3]$$

where

$$\mathrm{erfc}(i\omega) = \frac{2}{\sqrt{\pi}}\int_{i\omega}^{\infty} \exp(-t^2)\,dt \qquad [A4]$$

is the complementary error function, and ω^2 can be expressed for the air in the soil pores by

$$\omega^2 = \frac{ik_0 r_2(\cos\psi + \beta)^2}{2} \qquad [A5]$$

In Eq. [A5], $\beta = 1/Z$ where the impedance $Z(f)$ is given by Eq. [2]. Equation [A5] is valid for locally reacting soils in which sound is strongly refracted towards the normal at the air-soil boundary.

Excess Attenuation

The difference between P_{tot} and direct sound pressure levels at either of the receivers in Fig. 1a is called excess attenuation. That is the pressure received at the microphone location and above the effects of the geometric spreading of sound. Strictly, the influence of atmospheric absorption should also be considered, but will be negligible for the short ranges employed here. When both source and receiver are above the ground surface, the excess attenuation (in dB) can be expressed as

$$EA = 20\log_{10}\left|\frac{\frac{\exp(ik_0 r_1)}{r_1} + Q\frac{\exp(ik_0 r_2)}{r_2}}{\frac{\exp(ik_0 r_1)}{r_1}}\right| \qquad [A6]$$

If the direct and reflected rays are in phase, then the sound from the two rays will add coherently, causing constructive and destructive interferences, thus creating peaks and dips in the EA spectrum. If the waves have a phase difference of 180°, destructive interference occurs. The sound waves cancel each other and a dip or minimum in the EA spectrum is created. To calculate EA, a knowledge of the speaker out-

put is required—in other words, the contribution of a direct sound wave as if there was no ground surface present. This is known as a free field.

Level Difference

Level difference is the difference in pressure between the two vertically separated microphones, and is equal to the total field at the upper microphone minus the total field at the lower microphone. This can be expressed as

$$P_{\text{diff}} = 20 \log_{10} \left| \frac{\dfrac{\exp(ik_0 r_{1t})}{r_{1t}} + Q_t \dfrac{\exp(ik_0 r_{2t})}{r_{2t}}}{\dfrac{\exp(ik_0 r_{1b})}{r_{1b}} + Q_b \dfrac{\exp(ik_0 r_{2b})}{r_{2b}}} \right| \quad [A7]$$

where Q_t and Q_b are given by Eq. [3], [4], and [A2], with distances and angles appropriate to upper (subscript t) and lower (subscript b) receivers. The lower microphone's contribution acts as the direct ray and, thus, it is not necessary to know the source characteristics relative to free field. Ideally, the lower microphone should be positioned on the ground where $r_1 = r_2$, but, due to steep temperature gradients close to the ground, it is better to put it just above the ground surface, e.g., 0.10 m.

A typical experimental geometry in Fig. 1a is $H = 0.40$ m, $S = 1.75$ m, $h_1 = 0.10$ m, and $h_2 = 0.40$ m. This geometry is such that the first minimum (or impedance dip) in the EA spectrum at the lower microphone is outside the f range of interest, so its contribution does not complicate the level difference spectrum unduly.

REFERENCES

Attenborough, K. 1983. Acoustical characteristics of rigid fibrous absorbent and granular materials. J. Acoust. Soc. Am. 73:785–799.

Attenborough, K. 1985. Acoustical impedance models for outdoor ground surface. J. Sound Vib. 99:521–544.

Attenborough, K., and H.M. Hess. 1985. Acoustical surveying of porous soils. Acoust. Imaging 14:111–122.

Attenborough, K., J.M. Sabatier, H.E. Bass, and L.N. Bolen. 1986. The acoustic transfer function at the surface of a layered poroelastic soil. J. Acoust. Soc. Am. 79:1353–1358.

Avery, B.W., and C.L. Bascombe (ed.). 1982. Soil survey laboratory methods. Soil Survey, Harpenden, UK.

Chien, C.F., and W.W. Soroka. 1980. A note on the calculation of sound propagation along an impedance surface. J. Sound Vib. 69:340–343.

Grover, R.L. 1955. Simplified air permeameters for soil in place. Soil Sci. Soc. Am. Proc. 19:414–418.

Hess, H.M. 1988. Acoustical determination of physical properties of porous grounds. Ph.D. diss. Open Univ., Milton Keynes, UK.

Hillel, D. 1982. Introduction to soil physics. Academic Press, London.

Janse, A.R.P. 1969. Sound absorption at the soil surface. Cent. Agric. Publ. Doc., Wageningen, the Netherlands.

Kinsler, L.E., A.R. Frey, A.B. Coppens, and J.V. Sanders. 1980. Fundamentals of acoustics. 3rd ed. John Wiley & Sons, New York.

Kirkham, D. 1947. Field methods of determination of air permeability of soils in its undisturbed state. Soil Sci. Soc. Am. Proc. 11:93–99.

Kummer, F.A., and A.W. Cooper. 1945. Soil porosity determinations with the air pressure pycnometer as compared with the tension method. Agric. Eng. 26:21–23.

Leonard, R.W. 1946. Simplified flow resistance measurement. J. Acoust. Soc. Am. 17:240.

Meyer, L.D., and W.C. Harmon. 1979. Multiple-intensity rainfall simulator for erosion research on row sideslopes. Trans. ASAE 22:100–103.

Morse, P.M., and K.U. Ingard. 1986. Theoretical acoustics. Princeton Univ. Press, Princeton, NJ.

Officer, C.B. 1958. Sound transmission. McGraw-Hill Book Co., New York.

Page, J.B. 1948. Advantages of the pycnometer for measuring the pore space in soils. Soil Sci. Soc. Am. Proc. 12:81–84.

Pidgeon, J.D. 1974. A portable air pycnometer for rapid field measurement of air-filled porosity. Dep. Note DNSSN/169. Natl. Inst. Agric. Eng., Penicuik, Scotland.

Pierce, A.D. 1981. Acoustics. McGraw-Hill Book Co., New York.

Richards, T.L., K. Attenborough, N.W. Heap, and A.P. Watson. 1985. Penetration of sound from a point source into a rigid porous half-space. J. Acoust. Soc. Am. 78:956–963.

Russell, M.D. 1950. A simplified air-pycnometer for field use. Soil Sci. Soc. Am. Proc. 14:736–776.

Sabatier, J.M., H.E. Bass, L.N. Bolen, K. Attenborough and V.V.S.S. Sastry. 1986. The interaction of airborne sound with a layered poroelastic soil. J. Acoust. Soc. Am. 79:1345–1352.

Van der Haarst, G.G., and W.P. Stakman. 1965. Soil moisture retention curves II. i. Directions for use of the sand box apparatus, range pf 0 to 2.7. Inst. Land Water Manage. Res., Wageningen, the Netherlands.

Vomocil, J.A. 1965. Porosity. p. 299–314. *In* C.A. Black et al. (ed.) Methods of soil analysis. Part 1. ASA, Madison, WI.